Melt-mineral-fluid interaction in peralkaline silicic intrusions in the Oslo Rift, Southeast Norway. IV: Fluid inclusions in the Sande nordmarkite

TOM ANDERSEN

Andersen, T. 1990: Melt-mineral-fluid interaction in peralkaline silicic intrusions in the Oslo Rift, Southeast Norway. IV: Fluid inclusions in the Sande nordmarkite. *Nor. geol. unders. Bull. 417*, 41-54.

The mildly peralkaline Sande nordmarkite (quartz syenite) intrusion contains interstitial quartz and mafic minerals (alkali pyroxene, alkali amphibole, ilmenite, titanomagnetite, zircon, sphene + calcite). Three generations of fluid inclusions have been recognized in the interstitial quartz: primary inclusions (population 1), early secondary inclusions (population 2) and late secondary inclusions (population 3). Population 1 and 2 inclusions contain fluids which can be approximated by the H_2O-NaCl system, and were probably derived from the magma. The salinity of these fluids is ca. 40 wt% NaCl, but the fluids show a considerable variation in density (d = 0.9 to > 1.1 g/cm³), increasing with time and decreasing temperature. Population 3 fluids show complex immiscibility relationships involving vapour, highly saline liquids and solid salts. Also, low-salinity, high-density fluids of external origin become important at this stage.

Tom Andersen, Mineralogical-Geological Museum, Sars gate 1, N-0562 Oslo 5, Norway

Introduction

Volatile components (H_2O, CO_2, etc.) are important minor constituents in silicate magmas (e.g. Carmichael et al. 1974, Burnham 1979). During sub-surface crystallization, a magma may become saturated in volatiles, resulting in the evolution of a separate fluid phase (Holloway 1981). The pressure- temperature-composition evolution of fluids in a magmatic system may best be studied in fluid inclusions in its rock-forming minerals. The use of fluid inclusions in the study of plutonic rocks and their cooling histories have been reviewed by Weisbrod (1981) and Roedder (1984).

Some work has been devoted to the fluid evolution of alkaline or sub-alkaline, biotite-bearing granitic rocks in the Permo-Carboniferous Oslo region in Southeast Norway (Olsen & Griffin 1984a,b, Martinsen 1987), but little is known about the fluid regime in the peralkaline, acid intrusive rock in the area, such as nordmarkite (quartz syenite) (Andersen 1988). The present study and companion papers by Hansteen & Burke (1989) and Andersen et al. (1989) give the first information on the fluid evolution on these intrusions, based on fluid inclusion studies.

The present paper aims at establishing a fluid-rock interaction history for the Sande nordmarkite, based on microsocopy, supplemented by pertinent microthermometric measurements. Results from bulk fluid extraction analysis are presented by Andersen et al. (1990).

The Sande nordmarkite intrusion

The Sande nordmarkite intrusion forms part of the central pluton of the Sande Cauldron in the Permo-Carboniferous Oslo Rift in Southeast Norway (Fig. 1). The Sande Cauldron is one of a series of cauldron structures in the Oslo region, and probably represents a deeply eroded central volcano (Ramberg & Larsen 1978). The central pluton is zoned, with a monzonitic core enclosed by the nordmarkite. These two rock types represent different intrusive episodes, the nordmarkite postdating the monzonitic rocks (Andersen 1981, 1984a,b). Detailed petrographic descriptions and mineralogical data, as well as major- and trace-element analyses of the Sande nordmarkite were given by Andersen (1984 a,b) and Rasmussen et al. (1988).

The nordmarkite is a coarse-grained (0.5-1 cm grain size) alkali syenite, with a greyish-red colour and a well developed interstital micro-

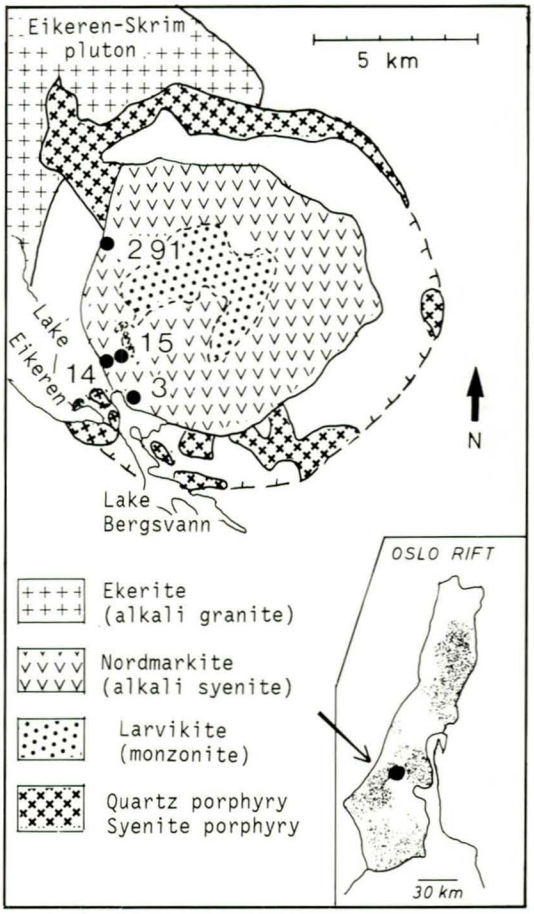

Fig.1. Simplified geological map of the Sande cauldron central pluton, from Andersen (1984a), with localities for the microthermometry samples, identified by numbers only (initial R or A omitted). Rhomb porphyry lavas within the cauldron block and the country rocks outside the cauldron (Lower Paleozoic sediments and Permo-Carboniferous lavas) are left without ornament.

structure. The modal quartz content varies from nil in the inner parts of the intrusion to > 10% in a marginal zone. The quartz-rich variety is typically porphyritic, and somewhat finer-grained than the quartz-free variety; the transition from quartz-bearing into quartz-free nordmarkite is completely gradual (Andersen 1984a). The predominant feldspar of the nordmarkite is sericitized mesoperthite, but rare, homogeneous grains of microcline are also found. Resorbed phenocrysts of plagioclase are moderately abundant in the porphyritic variety. Mafic silicates are interstitial dark green pleochroic clinopyroxene and pale (alkali or alkali-calcic) amphibole which are commonly intergrown with each other. Titanomagnetite and manganiferous ilmenite occur both interstitially and as inclusions in feldspar, and are commonly surrounded by biotite coronas. Close to the southern margin of the intrusion, mafic silicates are strongly altered to pseudomorphic aggregates of chlorite, serpentine and ferric hydroxide, with a few relics of the primary minerals. The most important accessory phases are zircon, sphene and apatite.

Miarolitic cavities are much less abundant in the Sande nordmarkite than in some other Oslo region plutons (e.g. Raade 1972). However, the nordmarkite contains abundant single or interconnected, open interstices, suggesting the presence of a fluid phase in the pluton at solidus and early sub-solidus temperatures. Some interstices are lined with epitaxial albite overgrowths on the surrounding feldspar; others contain zoned pyroxene and amphibole which have grown as euhedral crystals from nucleation points on the feldspar surfaces. Commonly, several interconnected, adjacent interstices are filled by optically continuous, anhedral quartz, postdating the other interstitial phases. In some samples from the southern margin of the intrusion, close to the contact towards Paleozoic sedimentary rocks, Fig. 1), calcite also occurs as an interstitial phase. These observations suggest that mineral growth from the interstitial fluid phase has been an important process in this pluton.

Although most of the quartz grains in the nordmarkite are free of inclusions of magmatic minerals (feldspar, pyroxene, opaque oxides), a few such grains have been located in sample A 14, where inclusions of cpx and opaque oxides outline euhedral growth zones. Alkali feldspar does not occur as inclusions in these quartz crystals. The zoned quartz crystals must have grown at the same time as the minerals found as solid inclusions.

Fluid inclusions

In most samples, the quartz contains great numbers of fluid inclusions of variable size, shape, mode of occurrence and phase contents at room temperature. The feldspar does not contain fluid inclusions, whereas apatite only contains a few late secondary inclusions.

The fluid inclusions can conveniently be classified according to their *phase contents at room temperature* (T_R, abbreviations used in

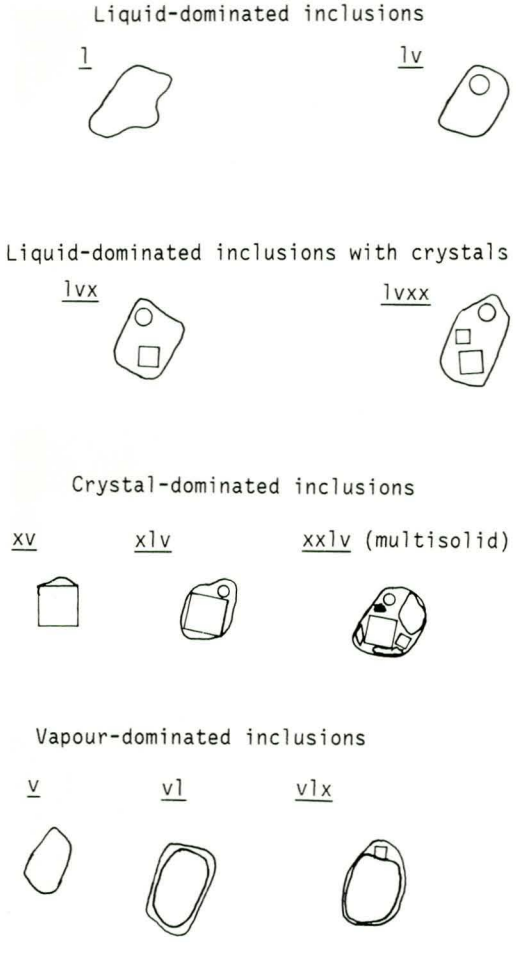

Fig. 2. Schematic illustrations of the types of fluid inclusions found in quartz from the Sande nordmarkite, as distinguished from phase content at T_R. The system of nomenclature used is defined in the text.

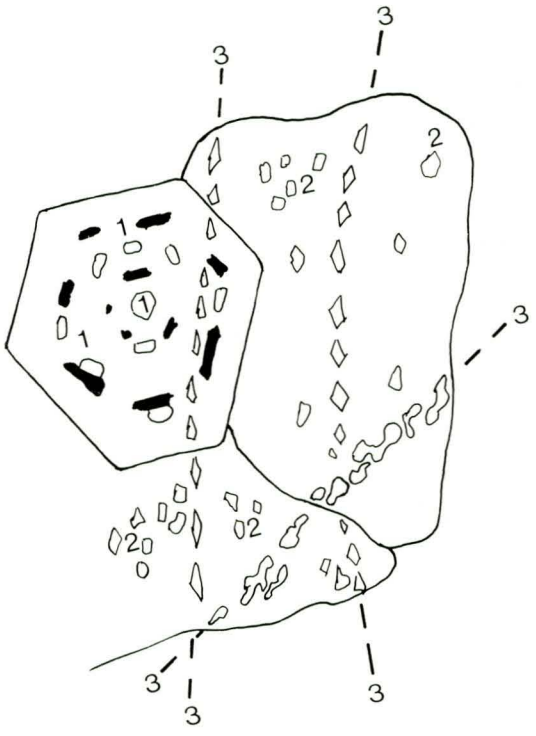

Fig. 3. Sketch showing the three different textural populations of fluid inclusions in the interstitial quartz: 1 Primary fluid inclusions occurring in zoned quartz, together with primary inclusions of magmatic minerals (black). 2 Fluid inclusions with no easily recognized relationship to either primary crystal growth zones or to secondary, healed fracture trails. 3 Secondary fluid inclusions occurring along healed fracture trails, postdating 1 and 2.

Table 1. Abbreviations

T_R	Room temperature (ca. 20° C)
T_{m1}	First melting temperature of the aqueous phase
T_{m,CO_2}	Melting point of CO2
$T_{m,Hh}$	Disappearance of hydrohalite
T_m	Final melting temperature
T_F	Filling temperature
$T_{d,NaCl}$	Dissolution of halite
$T_{d,x}$	Dissolution of unspecified crystals
T_h	Total homogenization temperature
T_{dec}	Decrepitation temperature
d	Density (g/cm³)
w_s	Salinity (equvalent weight percent NaCl)
l	Liquid phase in inclusion
v	Vapour phase in inclusion
x(x)	Solid phase(s) in inclusion

this paper are defined in Table 1) and their *textural setting within the quartz crystals.* This leads to a nomenclature which has both compositional and genetic significance (Figs. 2 and 3).

Phase contents at room temperature

The system of abbreviations used to describe the phase contents of the inclusions is based on the presence of liquid (l), vapour (v), one or several crystal(s) (x, xx) and their relative proportions at T_R. The most abundant phase is always mentioned first. Thus, lvx denotes a liquid-dominated three-phase fluid inclusion with a vapour bubble and one crystal.

Using this system, the inclusions can be divided into four classes, according to their

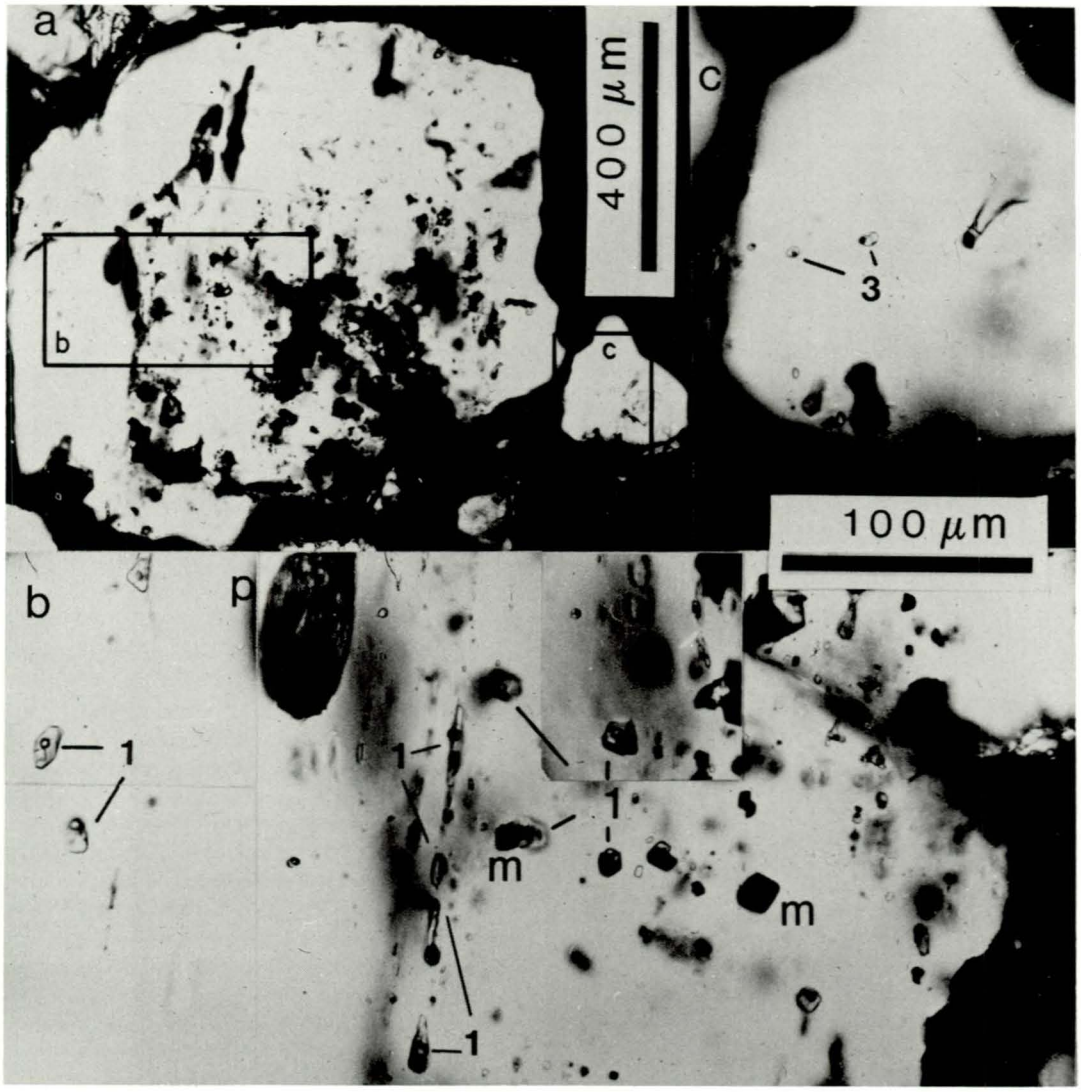

Fig. 4. Zoned interstitial quartz crystal in sample A 14. The 100 μm scale bar is common to b and c. Inclusions belonging to different textural populations are identified by single numbers (1, 3). a: Overall view of the quartz crystal. The localization of frames b and c are indicated. b: Composite of several, differently focused exposures of a part of the crystal. All fluid inclusions shown in this frame belong to population 1. p= pyroxene inclusions, m= magnetite inclusions. c: A secondary trail of multisolid xxlv fluid inclusions. These inclusions belong to population 3.

dominant phase at T_R as illustrated schematically in Fig. 2: (i) Liquid-dominated one- or two-phase inclusions without solids (l, lv). (ii) Liquid-dominated inclusions with 1-2 crystals (lvx, lvxx). (iii) Solid-dominated inclusions, consisting of a large proportion of solid(s) with a vapour phase (xv) and, most commonly, a liquid phase (xlv). Most of the solid-dominated inclusions are multisolid, containing several crystals with different optical properties (xxlv). (iv) Vapour-dominated inclusions (v, vl, vlx).

Distribution and chronology of fluid inclusions

The scarcity of growth zonation in the interstitial quartz complicates the process of deriving a chronological sequence of inclusion trap-

ping. A rough inclusion chronology can be defined from a study of local inclusion textures, as illustrated in Fig. 3. Rather than relating single inclusions or compositional types to distinct events in the evolution of the quartz, the inclusions have been grouped into three populations with a chronological significance. The inclusions range from the obviously early, truly primary inclusions (population 1) to the obviously late, secondary inclusions (population 3), with the fluid inclusions, which occur neither in recognizable growth zones nor along healed fractures making up a population 2.

Population 1. The only inclusions which fulfil the criteria of a primary origin (e.g. Roedder 1984) are found in zoned quartz crystals. These crystals contain fluid inclusions (lvx, with degree of fill < 0.9) attached to solid inclusions, or as separate negative crystals within clear zones of the crystal (Fig. 4). This is the earliest generation of fluid inclusions recognized, and the only ones which may give information on solidus or near-solidus fluids in the pluton.

Population 2 inclusions are scattered throughout unzoned quartz crystals, without any relationship to solid inclusions of magmatic minerals, or they are found in smaller groups or clusters (Fig. 5). This category probably includes inclusions of both primary and secondary origin, and is the largest group in terms of number of inclusions; lvx and lvxx inclusions are the most abundant types: Multisolid xxlv and vapour-dominated v, vl and vlx inclusions also occur, but only in subordinate numbers. Within single domains, or in clusters of population 2 lvx(x) inclusions, phase contents and liquid-solid-vapour abundances at T_R are generally quite similar (Fig. 5c). The population 2 inclusions were probably trapped over a large part of the cooling history, and there may be temporal overlap with both the primary population 1 and the obviously secondary population 3.

Population 3 comprises those inclusions which delineate recognizable healed fracture trails in the crystals. Their shapes vary from equant negative crystals (Fig. 6a) to anhedral and vermicular ones (Fig. 6b). Their characteristic occurrence implies that population 3 inclusions postdate population 1 inclusions and, in most

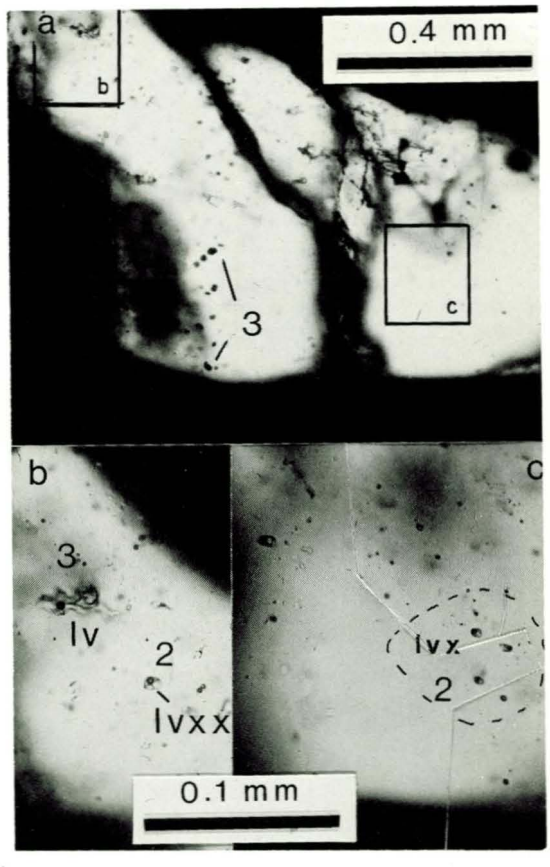

Fig. 5. Quartz crystal with population 2 and 3 fluid inclusions. The 100 μm scale bar is common to b and c. a: Overall view. The localization of frames b and c are indicated. Note a trail of population 3, vapour-dominated fluid inclusions. b: Detail showing population 2 lvxx inclusion and a high-density, irregular population 3 lv inclusion. c: Detail composed of two differently focused exposures, showing a group of population 2 lvx fluid inclusions.

cases, nearby clusters of population 2 inclusions. Two different associations of fluid inclusions dominate the population 3 trails: (i) Large, equant vapour-dominated inclusions (v, vl, vlx) associated with more irregular, xv or multisolid xxlv inclusions (Fig.6a). Solid and vapour-dominated types are generally found within one and the same inclusion trail, but xxlv inclusions are also found as the only type occurring in a trail (Fig. 4c). These trails cross-cut population 2 clusters, but are themselves cut by (ii) trails with lv or l inclusions (Fig. 6b) which represent the very last stage of fluid evolution recognized in the Sande nordmarki-

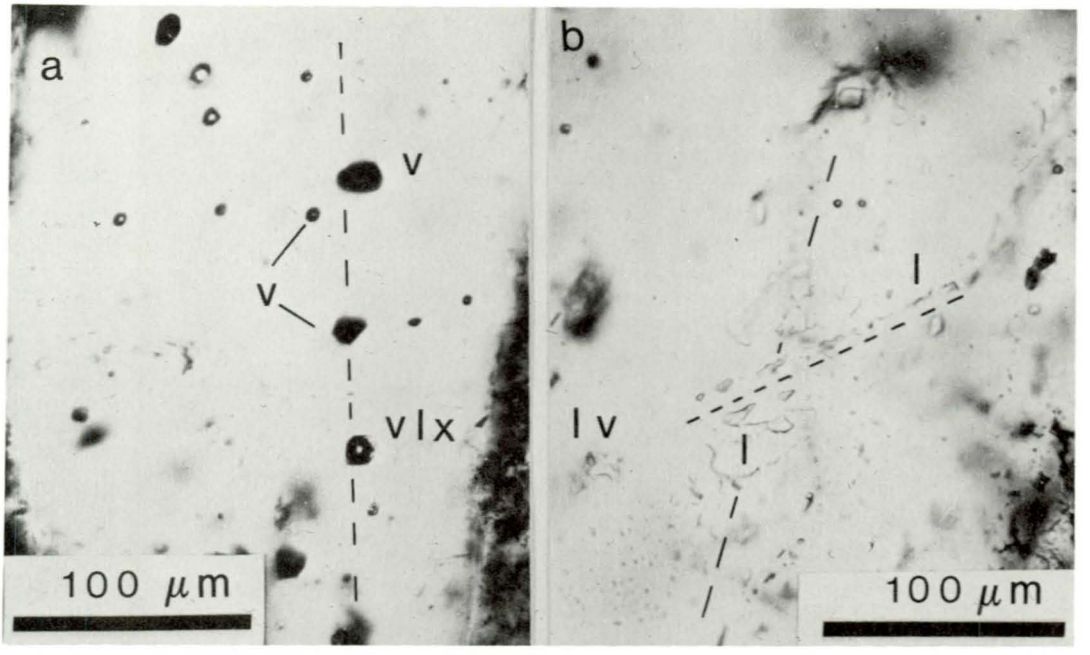

Fig. 6. Two different types of population 3 inclusion trails: a: Trail with regularly shaped v and vlx fluid inclusions. b: Two trails with irregular l and lv fluid inclusions. These trails cross-cut trails like the one illustrated in a, as well as all other fluid inclusion textures in the nordmarkite quartz.

te. In quartz from the southern margin of the intrusion, such late population 3 lv inclusions are the only fluid inclusions found. Sample A3 shows an example of such a fluid inclusion pattern; in this sample the mafic silicates are thoroughly altered, and calcite occurs as an interstitial phase.

The high-density, low-salinity population 3 l and lv fluid inclusions represent samples of a fluid phase which must be significantly different in terms of salinity and density from the earlier inclusion generations. Because of their high density, these inclusions show a much stronger tendency to decrepitate on heating than do the earlier, less dense inclusions. This is a nuisance during microthermometric analysis, but has the advantage that the bulk fluid extracted from a sample at T< 650° C will be dominated by these inclusions. Alkali thermometry on extracted fluids give temperature estimates in the interval 200-300° C (depending on the choice of thermometer, Andersen et al. 1990), suggesting that the population 3 l and lv fluid inclusions formed within this temperature interval, probably as a result of influx of externally derived (meteoric) water.

Identity of solid phases

No microanalytical methods have been employed in the present study; solids have therefore been tentatively identified from their optical properties and low-temperature behaviour. Four different types of crystals may be recognized: (i) *Isotropic cubes,* which are ubiquitous in lvx(x), vlx and solid-dominated inclusions (xlv, xxlv). One or two crystals are present, and the largest of these (the only one present in lvx) shows formation of a salt-hydrate at T<0°C; this in turn breaks down close to 0°C (several repeated cooling and heating cycles below 0°C may be needed to form the hydrate). This behaviour is characteristic for halite (NaCl) forming hydrohalite ($NaCl{=}2H_2O$) at low temperature. The other, smaller, isotropic cube is inert on cooling, and dissolves before halite on heating. This mineral is tentatively identified as sylvite (KCl).

(ii) *Weakly birefringent crystals.* These crystals are rhombohedral to irregular in shape, and dominate the xv and multisolid xlv inclusions. The interference colours are characteristically first-order grey. Similar crystals have been

found in fluid inclusions in quartz from the Eikeren alkali granite, where they have been identified by microanalytical techniques (Laser-Raman microprobe, EDS-SEM analysis) as various types of alkali sulphate daughter minerals and accidentally trapped amphiboles and feldspars (Hansteen & Burke 1989).

(iii): *Strongly birefringent grains.* The xxlv inclusions invariably contain one grain of a strongly birefringent mineral in addition to halite and weakly birefringent crystal(s). These are typically much smaller than any of the former types of crystals, but nevertheless show high-order interference colours. The optical properties suggest that the crystals are carbonates; calcite, dolomite and nahcolite ($NaHCO_3$) are likely candidates.

(iv): *Opaques.* Minute opaque grains have been observed in some xxlv inclusions. No positive identification is possible, but iron oxides or sulphides are the most likely possibilities.

Microthermometry

Based on a microscopic survey of the sample collections of Raade (1973) and Andersen (1981), four samples were selected for microthermometrical work. The petrographic characteristics of the samples are summarized in Table 2. The samples cover a considerable range in mafic mineralogy, geochemistry and pyroxene- and amphibole-compositions (cf. Andersen 1984a, Rasmussen et al. 1988).

Measurements have been concentrated on population 1 and 2 inclusions, which are relevant for the early sub-solidus cooling history of the pluton. Population 3 inclusions are under-represented in the data-set, because it was felt that the bulk fluid analyses presented by Andersen et al. (1989) were sufficient to delimit the trapping conditions of these inclusions to T< 300° C.

Table 2. Petrographic characteristics of microthermometry samples.

	Feldspar	Mafic silicates	Fe-Ti oxides	Accessories	Fluid inclusions
A 3	Perthite, plagioclase	Chlorite, serpentine, relict amphibole	Ferric hydroxides	Zircon, sphene, apatite, calcite	Population 3 only
A 14	»	Pyroxene, amphibole	Titanomagnetite, ilmenite	»	Population 1,2,3
A 15	»	»	»	»	Population 2,3
R 291	Perthite	»	»	»	Population 2,3

Experimental procedure

Microthermometric measurements on doubly polished sections were made with different types of combined heating-freezing stages. All the low-temperature work was carried out on a gas-cooled CHAIXMECA stage at the Mineralogical-Geological Museum, Oslo. The same stage was also used for most of the high-temperature work (T< 500°C), a LINKAM THM 600 stage was, however, used for some of the high-temperature runs (T< 600°C). A few measurements at T> 600°C were done with a USGS/Reynolds gas-heated stage at the Instituut voor Aardwetenschappen, Vrije Universiteit, Amsterdam. Detailed descriptions of these heating-freezing stages have been given by Shepherd et al. (1985). The stages were calibrated according to the procedures of Roedder (1984) and Andersen et al. (1984), using a selection of pure compounds with known melting points.

Microthermometric behaviour

The microthermometric behaviour of fluid inclusions is a function of composition and density, and thus depends upon the T_R phase content of the inclusions. Since the filling temperature (T_F) is the only phase transition common to all inclusion subgroups, the measurements are plotted against T_F in Fig. 7.

On cooling to $T<<T_R$, the liquid-dominated inclusions froze to an assemblage of ice, salt hydrate(s) and vapour. Typically, cooling to +60° C was needed to obtain total solidification of the inclusions.

First melting (by breakdown of a salt hydrate phase) took place at T_{m1} in the interval +50° to +25° C. In many inclusions, first melting was difficult to observe, and very often only a maximum limit for Tm1 could be determined.

Hydrohalite melting. In the lv inclusions, another hydrate phase (hydrohalite) broke down at $T_{m,Hh}$ between +30° and +25° C, leaving an assemblage of liquid + ice + vapour. The xxlv inclusions transformed to a mush of salt hydrate(s), original crystals and vapour at low T. Commonly, several repeated temperature cycles between 0 and ≈+60° C were necess-

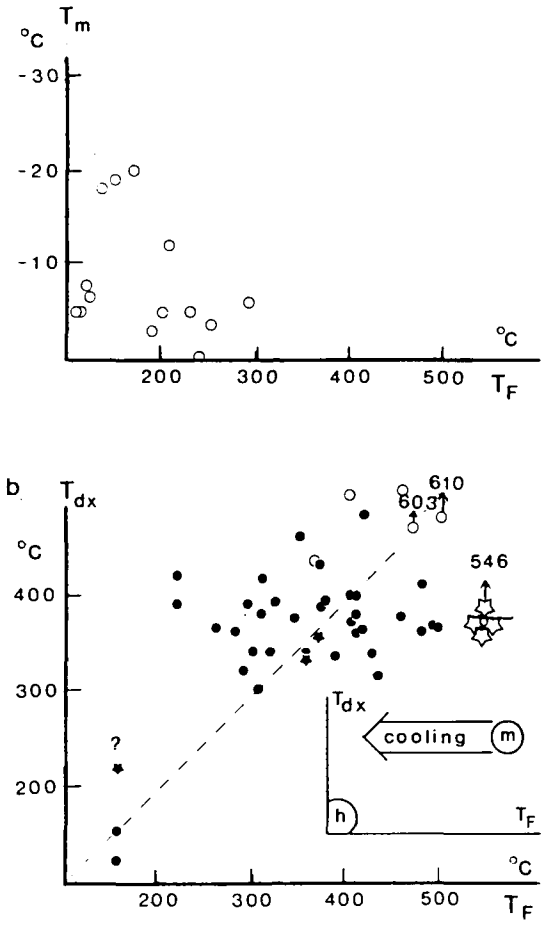

Fig. 7. Microthermometric measurements, plotted against the filling temperature. Stars: Population 1 inclusions (filled: T_F observed, open: decrepitated before T_F). Points: Population 2 inclusions. Circles: Population 3 inclusions. a: Final melting point of ice in Iv inclusions. b: Halite dissolution temperature. The broken line separates inclusions homogenizing by vapour bubble disappearance (lower right) from inclusions homogenizing by halite dissolution (upper left). Inset: trajectory of a magmatic fluid (initially within the circle m) during cooling in a closed system witin the single-phase region of an aqueous fluid. The circle h represents low-temperature hydrothermal fluids of meteoric origin.

.ary to transform all convertible salt to salt hydrate. Although sluggish, the final breakdown of the salt hydrate took place close to 0° C, leaving liquid + vapour + several grains of halite. The halite grains coalesced into a single salt cube on gentle heating.

Ice melting. In Iv inclusions, the ice disappeared at the final melting temperature (T_m), typically between +20° and +5° C (Fig. 7a). In Ivx inclusions, ice disappeared around +20° C, leaving hydrohalite (disequilibrium NaCl) + liquid + vapour.

CO_2-melting. When the vapour-dominated (vlx) inclusions were cooled to T< +80° C a second solid phase formed from the vapour; this solid melted abruptly close to the triple point of CO_2 (+56.6° C). No melting interval or depression of T_{m,CO_2} was observed. The homogenization of the gas phase could not be clearly observed, but took place below the final melting temperature of the water phase. The density of the CO_2 must therefore be very low, < 0.1 g/cm³ (e.g. Angus et al. 1973).

Filling and crystal dissolution. In Iv inclusions, only one high-temperature phase transition could be observed: homogenization to the liquid at $T_h = T_F$. In some Ivx and Ivxx inclusions, the solid(s) dissolved in the presence of liquid and vapour, leaving a two-phase (liquid + vapour) assemblage, which homogenized to the liquid at $T_h = T_F > T_{d,NaCl}$. In other Ivx, Ivxx and in solid dominated (xlv, xxlv) inclusions, the vapour-bubble disappeared before dissolution of the solid(s). Final homogenization took place by crystal dissolution at $T_h = T_{d,x} (=T_{d,NaCl}) > T_F$. Both types of homogenization behaviour may be observed for inclusions within one single quartz crystal, or even within a single domain in a crystal.

Composition and density of the fluid inclusions

Dissolved species. The predominance of halite in the solid-bearing inclusions show that Na^+ is an important cation in the fluid system. The low first-melting temperatures observed in Iv inclusions (T_{m1} = +50° to +25° C) indicate the presence of additional divalent metal ions in these inclusions, such as Ca^{2+}, which would give eutectic melting at ca. +50° C (Crawford 1981). Estimates based on $T_{m,Hh}$ between +30 and +25° C, suggest molar Na^+ / Ca^{2+} ratios in the range 0.8 - 1.9 in the late fluids trapped in the population 3 Iv inclusions (e.g. Shepherd et al. 1985). Although halite is the last phase to dissolve on heating in the multisolid xxlv inclusions, the presence of other crystals at T_R shows that other dissolved species than Na^+ and Cl^- are also present in these inclusions. These inclusions can probably best be described in terms of the components Na^+-

Ca^{2+}-K^+-Cl^--SO_4^{2-}-CO_3^{2-}, with NaCl as the dominant species.

ii: *Gas species.* There are no indications of free CO_2 in the vapour phase in any of the liquid-dominated inclusions. The gas-dominated inclusions (v, vl, vlx), however, contain low-density CO_2 with a melting point within experimental error of the triple point of pure CO_2. This suggests that the gas phase does not contain low-melting contaminants such as CH_4, N_2, etc. in concentrations above their detection limits (Burrus 1981, Touret 1982).

iii: *Salinities and densities.* The microthermometric data may be interpreted in terms of equivalent NaCl salinity and density by comparison with the relevant experimental data on H_2O-NaCl phase equilibria. The accuracy of this interpretation decreases as the number of solid phases at T_R increases: for lv and l inclusions the equivalent NaCl salinity ($w_{s)}$ can be determined from T_m, using an equation relating melting point depression to salinity (Potter et al. 1978). The density of lv inclusions can be estimated from w_s and T_h, using the experimental data of Zhang & Frantz (1987). The salinities of lv inclusions range from 0 to ca. 23 wt% NaCl (Fig. 8), with densities between 0.8 and 1.1 g/cm³. The densities of l inclusions are necessarily high (> 1 g/cm³, and cannot be determined accurately.

w_s of lvx and lvxx inclusions with $T_h = T_F$ can be determined from $T_{d,NaCl}$, using the equation for the three-phase liquid + vapour + halite curve in the binary system given by Potter et al. (1977). These inclusions homogenize at bubble-point curves corresponding to their w_s. The densities of these inclusions may be estimated from the empirical equation of Zhang & Frantz (1987), or by interpolation in a density-contoured w_s - T_h diagram (Bodnar 1983, Fig. A1).

In lvx, lvxx and xxlv inclusions with $T_h = T_{d,NaCl}$, halite dissolves on a liquidus (fluid + solid) curve above the three-phase region. The salinity may thus be determined by comparison with the data of Gunter et al. (1983). For the multisolid inclusions, w_s may be a poor representation of the total concentration of dissolved ionic species at the homogenization temperature. As discussed by Roedder (1984) and Shepherd et al. (1985), T_F cannot be related directly to the density in such inclusions.

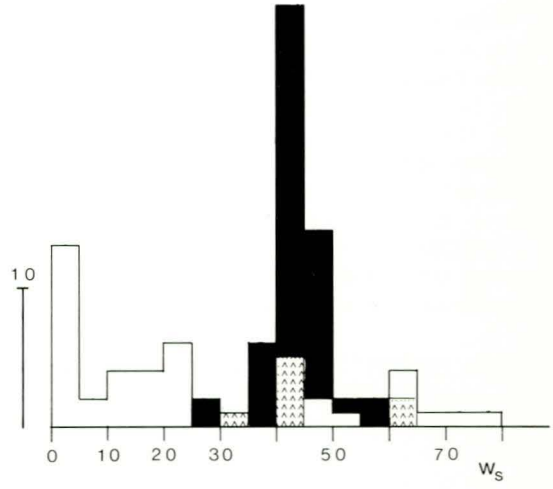

Fig. 8. Histogram of NaCl-equivalent salinity, calculated from microthermometric data. Shaded: population 1. Black: population 2. White: population 3.

The resulting distribution of inclusion salinities is shown in Fig. 8. The population 2 inclusions have a pronounced salinity maximum at ca. 40 wt% NaCl, regardless of homogenization temperature. The densities of the population 2 inclusions are in the range 0.9 to 1.1 g/cm³. The majority of population 1 inclusions available for study also have salinities close to 40 wt%, but most of them have higher homogenization temperatures, corresponding to d< 0.9 g/cm³ - with the exception of a single low salinity inclusion, which may be a wrongly identified population 3 inclusion (Fig. 7b).

The bulk composition and density of CO_2-bearing vl and vlx inclusions cannot be assessed quantitatively. It should, however, be noted that vlx and xv inclusions must have a total salinity above 25 wt% at a low total density.

Isochore calculation

Isochores for aqueous inclusions with moderate (<ca. 30 wt%) total salinity and $T_h = T_F$ can be calculated from the homogenization temperatures, using the empirical equations of Zhang & Frantz (1987). For such inclusions with higher salinities, approximate isochores can be constructed from data of Potter & Brown (1977) and Urusova (1975). Minor inconsistencies between the three sets of data should be expected.

Since the density of an inclusion homogenizing at a liquidus curve cannot be determined from microthermometric data, no isochores can be calculated for such inclusions. However, the isochore for any such inclusion is constrained within a PT sector between the pertinent bubble-point curve and fluid liquidus curve (e.g. Shepherd et al. 1985).

Selected isochores are shown in Fig. 9, together with other pertinent univariant phase equilibrium curves for the H_2O-NaCl system.

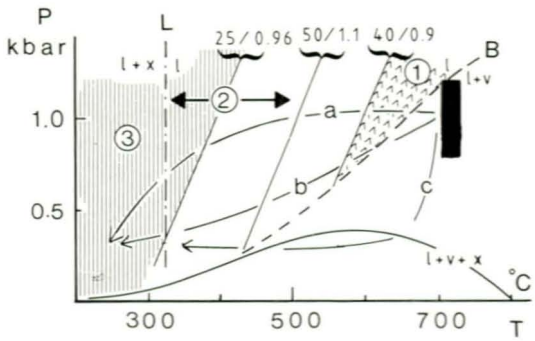

Fig. 9. PT interpretation of microthermometric data from the Sande nordmarkite. The figure shows the three-phase l + v + x curve of the H_2O-NaCl system (solid line) and the bubble-point curve of a 40 wt% NaCl solution (broken line labeled B) both from Bodnar et al. (1985). Isochores for H_2O-NaCl solutions (labelled with salinity (wt% NaCl) / density (g/cm³)) have been constructed from the data of Potter & Brown (1977) and Urusova (1975). The dash-dot line is a liquidus curve for a 40 wt% NaCl solution (labelled L), after Gunter et al. (1983). The black rectangle represents the inferred solidus conditions of the nordmarkite magma (700-720° C, 1.0 ± 0.2 kbar). Circled numbers (1, 2, 3) identify PT sectors of trapping conditions for population 1, 2 and 3 fluid inclusions, as discussed in the text; a, b and c are three different cooling PT paths for the fluid system in the Sande nordmarkite; a and b are allowed by the present fluid inclusion data, whereas c is not permitted.

Discussion

The fluid inclusions in the Sande nordmarkite have been trapped from fluids interacting with the cooling magma or solidified rock over a range of temperatures, from near the solidus to the far sub-solidus. The chronological sequence derived for fluid inclusions in the nordmarkite reflects the cooling history of the rock. From textural observations, only the primary population 1 inclusions are expected to give information about fluids present in the pluton near the solidus temperature. The younger generations of fluid inclusions (populations 2 and 3) represent fluids trapped at later stages of evolution; the late trails of population 3 l and lv inclusions reflect the very last fluid retained in inclusions in the quartz.

Trapping mechanism

The relationship between the composition and density of fluid inclusions in a plutonic rock and the properties of the magmatic or post-magmatic fluid phase may not always be straightforward (e.g. Roedder 1981, 1984, Weisbrod 1981). Overlooking the effects of heterogeneous trapping and post-trapping modification processes (e.g. leakage or necking down, Roedder 1981) can lead to erroneous interpretation of the compositional characteristics and PTX evolution of the fluid phase.

Deciding whether a given assemblage of fluid inclusions has been trapped from a homogeneous or heterogeneous fluid phase is always a major problem. Two types of heterogeneities are possible in saline aqueous fluids: (1) Halide (halite) saturation, or (2) immiscibility between two fluid phases (boiling, effervescence). The first phenomenon affects fluid inclusions trapped at temperatures at or below the relevant liquidus curve, whereas two immiscible fluids may be trapped within the two-phase liquid + vapour region. On the three-phase l +v + x curve, these two phenomena take place simultaneously.

Heterogeneous trapping of a solid-saturated fluid can be recognized by microscopy; the presence of coeval liquid- and halite-dominated inclusions within a single secondary trail or primary domains in a section is sufficient evidence that the fluid was saturated at the time of trapping. Observations of simultaneous inclusions with locally variable, relative liquid and vapour contents are necessary, but not sufficient, evidence for heterogeneous trapping of immiscible liquid and vapour phases, since mixing of fluids of different provenance may sometimes give similar textures. To distinguish splitting of a homogeneous fluid by liquid immiscibility from mixing of two (miscible) fluids, careful microthermometry is needed (Pichavant et el. 1982, Ramboz et al. 1982). However, for the purpose of the present discussion, it is important to note that *both* of these heterogeneous trapping mechanisms may usually be ruled out by microscopy. Uniform relative phase volumes within coeval groups of fluid inclusions are good evidence in favour of trapping from a homogeneous fluid.

Zones of population 1 lvx inclusions, and individual groups and clusters of population 2 lvx(x) inclusions show uniform relative phase volumes (Figs. 4, 5). This contradicts trapping from a heterogeneous fluid, and also suggests that the effects of post-entrapment modification processes (leakage, decrepitation, necking down) on the compositions and salinities of these inclusions have been negligible. The solid phases in the population 1 and 2 lvx(x) inclusions are therefore regarded as true daughter minerals rather than accidentally trapped solids. The composition and densities determined for the different groups or generations of inclusions reflect the properties of the fluid at the time of trapping.

A similar argument may be applied to the latest among the fluid inclusions in the samples: the late population 3 l and lv trails have internally uniform degrees of fill, and do not contain inclusions with aberrant properties. These trails must have been trapped from a homogeneous fluid.

The population 3 trails which predate the lv and l trails contain inclusions with different phase contents and degree of fill (lvx, xlv, vlx, vx). This indicates more complex trapping mechanisms, which involved two (l + x, possibly also l + v) or three (l + v + x) phases in the system. Such inclusions do not give a simple representation of the bulk composition of the fluid at the time of trapping.

P-T-X evolution of the fluid phase

In the following discussion, the H_2O-NaCl system will be used as a model for the high-temperature behaviour of the fluid phase in the Sande nordmarkite.

Near-solidus fluids. The population 1 inclusions contain an aqueous fluid, with w_s ca. 40 wt% NaCl and density less than 0.9 g/cm³. These inclusions homogenized either on the 40 wt% NaCl bubble-point curve, or they decrepitated before T_F was reached. Isochores for these inclusions extend from homogenization points on the bubble-point curve into a PT sector limited by this curve and the 40 wt% NaCl, 0.9 g/cm³ isochore (Fig. 9). The only feasible source for the fluid contained in these inclusions is the magma itself.

Based on analogies with quartz + feldspar + aluminosilicate melt equilibria in comparable experimental systems (Tuttle & Bowen 1958, Hamilton & MacKenzie 1965, Thompson & MacKenzie 1967), Andersen (1984a) estimated a solidus-temperature of 700-720°C for quartz-bearing nordmarkite. The lithostatic pressure during in-situ crystallization of the magma can only be assessed by comparison with the local geology. The Sande pluton has penetrated into top of the Lower Paleozoic sedimentary sequence of the Oslo region, and the lowermost Permo-Carboniferous lavas (Oftedahl 1953). In the southern part of the Oslo Region, the lava pile attains a maximum thickness of ca. 3000 m (Oftedahl 1978). This limits the lithostatic pressure during in-situ crystallization to ca. 1 kbar. In Fig. 9, P= 1.0+0.2 kbar, T= 700-720° C are adopted as solidus conditions. The hydrostatic pressure in a 3000 m high fluid column with d= 1.0 g/cm³ is 300 bar. This is a maximum estimate for the hydrostatic pressure in the Sande pluton shortly after its emplacement.

The inferred solidus PT conditions of the nordmarkite fall to the high-T, low-P side of the population 1 isochore sector; increasing the salinity of the system to 50 wt% NaCl shifts the low-P — high-T limit of the possible trapping conditions of the population 1 fluid inclusions towards high temperature, but only to give marginal improvement of the overlap with the estimated solidus conditions. However, it is a very real possibility that the outer zones of the zoned quartz grains and the aegirine and magnetite crystals included in them, may have grown from the aqueous fluid itself, rather than from a silicate melt proper. In his classical study of the stability of aegerine, Bailey (1969) reported evidence of aegirine and other mafic minerals having grown from a vapour phase. He also found that his experimental charges contained a liquid after quenching to room temperature. This liquid corresponded to a strongly alkaline aqueous fluid which coexisted with aegirine, quartz, magnetite etc. at experimental pressure and temperature, and was directly responsible for growth of silicate phases from 'vapour'. Such a fluid would have close similarity to that contained in the present population 1 fluid inclusions.

'Early' sub-solidus fluid. The fluid trapped in the population 2 lvx(x) inclusions has a salinity of ca. 40 wt% NaCl, which overlaps with the salinity of the near-solidus fluid contained in population 1 inclusions. This limited salinity range, and the textural evidence for trapping

from a single, homogeneous fluid phase suggest that the influence of externally derived fluids at this stage of evolution was moderate. However, the density of population 2 lvx(x) inclusions ranges from 0.9 to 1.1 g/cm³, yielding a broad sector of isochores in the PT-plane. In Fig. 9, the isochore of a fluid inclusion with 50 wt% NaCl and d= 1.1 g/cm³ defines the upper temperature limit for this field; the minimum temperature limit is given by the liquidus of a 40 wt% NaCl solution (Gunter et al. 1983). Below this liquidus curve, a 40 wt% NaCl solution would be saturated in halite, and homogeneous trapping of such a fluid would be impossible. The less dense fluid inclusions define isochores at higher temperatures than do the more dense. Given a uniform and continuous cooling path for the pluton, the less dense inclusions must have been trapped at higher temperatures or earlier than the more dense ones, regardless of the actual shape of the cooling path. An increase in density at constant salinity is what should be expected from a homogeneous fluid phase cooling within a closed system at P-T conditions within the single-phase region of the fluid composition in question. The response of homogenization temperature and halite dissolution temperature to closed system cooling is illustrated as an inset to Fig. 7b.

'Late' sub-solidus fluid. At the time the population 3 fluid inclusions were trapped, the fluid phase in the pluton was no longer homogeneous; textural evidence suggest that two- or three-phase immiscibility may have taken place, and that externally derived fluids became important at this stage, most likely as a result of onset hydrothermal circulation (Andersen et al. 1990). It should be noted that the 'magmatic' 40 wt% NaCl fluid would become saturated in halite on cooling below ca. 320°C (Gunter et al. 1983), making heterogeneous trapping of halite and aqueous fluid possible over a wide pressure range below this temperature. Furthermore, the present observations suggest that a CO_2-bearing low-density fluid was also present in the pluton at this stage. This fluid may have exsolved from the 'magmatic' aqueous fluid, or it may have been introduced from an external source, such as Lower Paleozoic limestones among the country rocks.

The maximum salinity observed among population 3 lv inclusions is ca. 25 wt% NaCl, with a corresponding density of 0.96 g/cm³ (Fig. 8). The isochore corresponding to such an inclusion is illustrated in Fig. 9; this isochore defines a maximum temperature limit for the trapping conditions of population 3 lv and l inclusions and intersects the the 40 wt% NaCl liquidus at 320° C, ca. 400 bar.

The cooling path

Although no method to estimate trapping pressure for different types of sub-solidus fluid inclusions is available, it appears safe to assume that a hydrostatic pressure regime was established by the time hydrothermal circulation had started and the trapping of lv and l inclusions took place ($T < 300°C$).

In Fig. 9, three alternative cooling paths leading from lithostatic pressure at the solidus to hydrostatic pressures at 300°C are shown. Closed-system cooling along an 'isobaric' PT path close to lithostatic pressure (i.e. path a in Fig. 9), or at decreasing pressures above the bubble-point curve of a 40 wt% NaCl solution (path b in Fig. 9) are permitted by the present fluid inclusion data, as they would not lead to heterogeneity phenomena within the trapping range of population 1 and 2 inclusions. If the bubble-point curve had been crossed, textural evidence of two-fluid immiscibility would have been expected.

The third path (c) illustrated in Fig. 9 represents a case of abrupt pressure-decrease to hydrostatic levels at near-solidus temperatures, akin to the evolution of many porphyry-type ore deposits (e.g. Roedder 1984). Given a starting-point of a 40 wt% NaCl solution above its bubble point curve at 700°C this path would lead to condensation of a liquid phase at temperatures very close to the solidus of the silicate melt (intersection with the 40 wt% bubble-point curve) and saturation with halite where cooling path c hits the l + v + x curve. Along this path, the liquid phase would have $w_s > 60$ wt% NaCl at the time halite saturation took place. Cooling along path c would lead to complex fluid inclusion assemblages characteristic of l + v or l + v + x *immiscibility / saturation at temperatures* where the present data show that the fluid phase in the Sande nordmarkite still remained homogeneous. This path thus cannot account for the fluid inclusion textures and compositions observed in the Sande nordmarkite. In this respect, the Sande pluton is similar to the

Drammen biotite granite pluton, where a lithostatic pressure regime has dominated, except in a marginal zone (Olsen & Griffin 1984a,b).

Implications

The Sande nordmarkite resembles several other evolved, acid plutons in the Oslo Region in having lower concentrations of LIL elements than expected from a fractional crystallization model (Dietrich et al. 1965, Dietrich & Heier 1965, Raade 1973, Andersen 1981, Rasmussen et al. 1988). In a magmatic system consisting of silicate melt, minerals and an aqueous fluid, trace elements will be distributed between crystals, melt and fluid, the solubilities of the elements determining their relative enrichment in the fluid phase (Neumann et al. 1989). In the Sande pluton, the magmatic fluid may have been retained within the rock body until the onset of hydrothermal circulation at ca. 300° C. The trace elements partitioned into the fluid phase during igneous crystallization may have been lost together with the remains of primary fluid at this stage.

Also, the radiogenic isotopic system of the nordmarkite may have been disturbed at this stage, by isotopic exchange with the country rocks *via* a migrant fluid phase. Rasmussen et al. (1988) reported new Rb-Sr data on the Sande pluton, showing that this intrusion does not define an isochron, in contrast to several other syenitic - granitic intrusions in the Oslo Region.

Conclusions

The fluid inclusions contained in interstitial quartz in the Sande nordmarkite are dominantly aqueous solutions (NaCl ± $CaCl_2$ ± KCl ± carbonate components ± sulphate components). 'Solidus' and early sub-solidus fluid inclusions were trapped from a homogeneous fluid phase which originated from a magmatic fluid (ca. 40 wt% NaCl) which cooled in a closed system within the rock body. The evolution of this fluid phase may be traced in inclusions from solidus temperatures (ca. 700°C). to 300°C, where immiscibility phenomena and influx of externally derived fluids may have become important. CO_2 occurs only in late secondary inclusions, and may have an external origin.

The cooling-path of the Sande nordmarkite pluton was confined within the single-phase region of a 40 wt% NaCl solution from the solidus to ca. 300°C. In this respect, the sub-solidus cooling history of the Sande nordmarkite intrusion is different from many porphyry-mineralized intrusions, where intense fracturing, immiscible splitting of magmatic fluid into liquid and vapour fractions and influx of externally derived fluids take place at temperatures much closer to the solidus (600-700°C).

Acknowledgements

The laboratory work was supported by the Norwegian Research Council for Science and Technology (Ores associated with Permian intrusives - Oslo region). The author wants to thank E.-R. Neumann, T.H. Hansteen, A.H. Rankin and J.L.R. Touret for numerous helpful discussions. Constructive criticism from J. Dubessy of an early version of the text is gratefully acknowledged.

References

Andersen, T. 1981: *En geokjemisk- petrologisk undersøkelse av de intrusive bergartene i Sande Cauldron, Oslofeltet.* Unpubl. Cand. real. thesis, University of Oslo, 321 pp.

Andersen, T. 1984a: Crystallization history of a Permian composite monzonite-alkali syenite pluton in the Sande cauldron, Oslo rift, S. Norway. *Lithos 17,* 153-170.

Andersen, T. 1984b: Hybridization between larvikite and nordmarkite in the Oslo region, S.E. Norway: A case study from the Sande Cauldron central pluton. *Nor. Geol. Tidsskr. 64,* 221-233.

Andersen, T. 1988: Sub-solidus fluidutvikling i Sande nordmarkitten, Oslo riften, sydøst Norge (abstract) *18. Nordiske Geologiske Vintermøde, København 1988,* p. 24

Andersen, T., O'Reilly, S.Y. & Griffin, W.L. 1984: The trapped fluid phase in upper mantle xenoliths from Victoria, Australia: implications for mantle metasomatism. *Contrib. Mineral. Petrol. 88,* 72-85.

Andersen, T. Rankin, A.H. & Hansteen, T.H. 1990: Melt-mineral- fluid interaction in peralkaline silicic intrusions in the Oslo rift, SE Norway. III: Alkali geothermometry based on bulk fluid inclusion content. *Nor. geol. unders. Bull. 417,* 33-40.

Angus, S., Armstrong, B. & de Reuck, K.M. 1973: *International thermodynamic tables of the fluid state - 3: Carbon dioxide.* IUPAC Thermodynamic Tables Project, Pergamon Press, Oxford, 385 pp.

Bailey, D.K. 1969: The stability of acmite in the presence of H_2O. *Am. Jour. Sci. 267-A,* 1-16.

Bodnar, R.J., 1983: A method of calculating fluid inclusion volumes based on vapour bubble diameters and P-V-T-X properties of inclusion fluids. Econ. Geol. 78, 535-542.

Bodnar, R.J., Burnham, C.W. & Stephens, S.M. 1985: Synthetic fluid inclusions in natural quartz. III Determination of phase equilibrium properties in the system H_2O-NaCl to 1000° C and 1500 bars. *Geochim. Cosmochim. Acta 49,* 1861-1874.

Burnham, C.W. 1979: Magmas and hydrothermal fluids. *In* Barnes, H.L. (ed.): *Geochemistry of hydrothermal ore deposits (2nd. edition)* J. Wiley & Sons, New York, 71-136.

Burrus R.C. 1981: Analysis of phase equilibria in C-O-H-S fluid inclusions. *Mineral. Assoc. Canada, Short course handbook 6,* 39-74.

Carmichael, I.S.E., Turner, F.J. & Verhoogen, J. 1974: *Igneous petrology.* McGraw-Hill, New York, 739 pp.

Crawford, M.L. 1981: Phase equilibria in aqueous fluid inclusions. *Mineral. Assoc. Canada, Short course handbook 6,* 75- 100.

Dietrich, R.V. & Heier, K.S. 1965: Differentiation of quartz bearing syenite (nordmarkite) and riebeckite-arfvedsonite granite (ekerite) of the Oslo series. *Geochim. Cosmochim. Acta 31,* 275-280.

Dietrich, R.V., Heier, K.S. & Taylor, S.R. 1965: Studies on the igneous rock complex of the Oslo Region XX. Petrology and geochemistry of ekerite. *Skr. Norske Vitenskapsakad. Oslo, I Mat.-Naturv. Klasse Ny Serie 19,* 31 pp.

Gunter, W.D., Chou, I.-M. & Girsperger, S. 1983: Phase relations in the system NaCl-KCl-H_2O. Part II: Differential thermal analysis of the halite liquidus in the NaCl-H_2O binary above 450° C. *Geochim. Cosmochim. Acta 47,* 863-873.

Hamilton, D.L. & MacKenzie, W.S. 1965: Phase equilibrium studies in the system $NaAlSiO_4$ (nepheline)-$KAlSiO_4$ (kalsilite)-SiO_2-H_2O. *Min. Mag. 34,* 214-231.

Hansteen, T.H. & Burke, E.A.J. 1990: Melt-mineral-fluid interaction in peralkaline silicic intrusions in the Oslo Rift, Southeast Norway. II: High-temperature fluid inclusions in the Eikeren-Skrim complex. *Nor. geol. unders. Bull. 417,* 15-32.

Holloway, J.R. 1981: Volatile interaction in Magmas. *In* Newton, R.C., Navrotsky, A. & Wood, B.J. (eds): *Thermodynamics of minerals and melts.* Springer Verlag, New York, 273-293.

Martinsen, M. 1987: *Den permiske metallogenese i Drammens-granitten, Oslofeltet: mineralogiske, geokjemiske, genetiske og strukturelle studier.* Unpubl. doctoral thesis, NTH, Trondheim, Norway, 202 pp.

Neumann, E.-R., Andersen, T. & Hansteen, T.H. 1990: Melt-mineral-fluid interaction in peralkaline silicic intrusions in the Oslo Rift, Southeast Norway. I: Geochemistry of the Eikeren Ekerite. *Nor. geol. unders. Bull. 417,* 1-13.

Oftedahl, C. 1953: Studies on the igneous rock complex of the Oslo Region. XIII The cauldrons. *Skr. Norske Vitenskapsakad. Oslo, I Mat.-Naturv. Klasse 1953 No. 3,* 108 pp.

Oftedahl, C. 1978: Main geologic features of the Oslo Graben. *In* Ramberg, I.B. & Neumann, E.-R. (eds.) *Tectonics and geophysics of continental rifts.* D. Reidel, Dordrecht, Holland, 149-160.

Olsen, K.I. & Griffin, W.L., 1984a: Fluid inclusion studies of the Drammen Granite, Oslo Paleorift, Norway. I. Microthermometry. *Contrib. Mineral. Petrol. 87,* 1-14.

Olsen, K.I. & Griffin, W.L. 1984b: Fluid inclusion studies of the Drammen Granite, Oslo Paleorift, Norway. II. Gas- and leachate analyses of miarolytic quartz. *Contrib. Mineral. Petrol. 87,* 15-23.

Pichavant, M., Ramboz, C. & Weisbrod, A. 1982: Fluid immiscibility in natural processes: Use and misuse of fluid inclusion data. I. Phase equilibria analysis A theoretical and geometrical approach. *Chem. Geol. 37,* 1-27.

Potter, II, R.W. & Brown, D.L. 1977: The volumetric properties of aqueous sodium chloride solutions from 0° to 500° C and pressures up to 2000 bars based on a regression of available data from the literature. *US Geol. Surv. Bull. 1421-C,* 36 pp.

Potter, II, R.W., Babcock, R.S. & Brown, D.L. 1977: A new method for determining the solubilities of salts in aqueous solutions at elevated temperatures. *US Geol. Surv. Jour. Res. 5,* 389-395.

Potter, II, R.W., Clynne, M.A. & Brown, D.L. 1978: Freezing point depression of aqueous sodium chloride solutions. *Econ. Geol. 73,* 284-285.

Ramboz,C., Pichavant, M. & Weisbrod, A. 1982: Fluid immiscibility in natural processes: Use and misuse of fluid inclusion data. II. Interpretation of fluid inclusion data in terms of immiscibility. *Chem. Geol. 37,* 29-48.

Ramberg, I.B. & Larsen, B.T. 1978: Tectonomagmatic evolution. *Nor. geol. unders. 337,* 55-73.

Rasmussen, E., Neumann, E.-R., Andersen, T., Sundvoll, B., Fjerdingstad, V. & Stabel, A. 1988: Petrogenetic processes associated with intermediate and silicic magmatism in the Oslo rift, southeast Norway. *Min. Mag. 52,* 293-307.

Raade, G. 1972: Mineralogy of the miarolitic cavities in the plutonic rocks of the Oslo region, Norway. *Mineral. Record 3,* 7-11.

Raade, G. 1973: *Distribution of radioactive elements in the plutonic rocks of the Oslo region.* Unpubl. cand. real. thesis, University of Oslo, 162 pp.

Roedder, E. 1981: Origin of fluid inclusions and changes that occur after trapping. *Mineral. Assoc. Canada, Short course handbook 6,* 101-137.

Roedder, E., 1984: *Fluid inclusions.* Reviews in Mineralogy 12, 644 pp.

Shepherd, T, Rankin, A.H. & Alderton, D.H.M. 1985: *A practical guide to fluid inclusion studies.* Blackie, Glasgow, 239 pp.

Thompson, R.N. & MacKenzie, W.S. 1967: Feldspar-liquid equilibria in peralkaline acid liquids, an experimental study. *Am. Jour. Sci. 265,* 714-734.

Touret, J.L.R., 1982: An empirical phase diagram for a part of the N_2-CO_2 system at low temperature. *Chem. Geol. 37,* 49-58.

Tuttle, O.F. & Bowen, N.L. 1958: Origin of granite in the light of experimental studies in the system $NaAlSi_3O_8$ - $KAlSi_3O_8$-SiO_2-H_2O. *Geol. Soc. Am. Mem. 74,* 153 pp.

Urusova, M.A. 1975: Volume properties of aqueous solutions of sodium chloride at elevated temperatures and pressures. *Russian Jour. Inorg. Chem. 20,* 1717-1721.

Weisbrod, A. 1981: Fluid inclusions in shallow intrusives. *Mineral. Assoc. Canada, Short course handbook 6,* 241-271.

Zhang, Y.-G. & Frantz, J.D. 1987: Determination of the homogenization temperatures and densities of supercritical fluids in the system NaCl-$CaCl_2$-H_2O using syntethic fluid inclusions. *Chem. Geol. 64,* 335-350.

Manuscript received November 1988; revised typescript May 1989; accepted July 1989.